Pickering emulsion gels based on halloysite nanotubes and ionic biopolymers: properties and cleaning action on marble surface.

Giuseppe Cavallaro,[1] Stefana Milioto,[1] Läysän Nigamatzyanova,[2] Elvira Rozhina,[2] Farida Akhatova,[2] Rawil Fakhrullin,[2*] Giuseppe Lazzara[1,*]

1   Dipartimento di Fisica e Chimica, Università degli Studi di Palermo, Viale delle Scienze, pad. 17, 90128 Palermo, Italy and Consorzio Interuniversitario Nazionale per la Scienza e Tecnologia dei Materiali, INSTM, Via G. Giusti, 9, I-50121 Firenze, Italy.

2   Institute of Fundamental Medicine and Biology, Kazan Federal University, Kreml uramı 18, Kazan, Republic of Tatarstan, 420008, Russian Federation. kazanbio@gmail.com

Abstract

We have fabricated ecocompatible Pickering emulsions based on halloysite nanotubes and ionic biopolymers (chitosan and pectin) from renewable resources. The effect of pectin and chitosan on the Pickering emulsion was investigated by direct visualization of the oil droplets and by the thermodynamic characterization at the interface. Pectin enhances the Pickering emulsion stability, while a phase separation and non-homogeneous gel was observed in the presence of chitosan. We have demonstrated that the Pickering emulsion in pectin based gel phase is suitable for wax layer removal from marble surface. A controlled cleaning is achieved by tuning the contact time between the gel and the marble surface. This work opens to new sustainable approach in preparing cleaning formulations for conservation of Cultural Heritage.

Introduction

Emulsions are widely used in cleaning protocols and they are particularly attractive in the conservation of Cultural Heritage. Oil-in-water emulsions present as the main advantage the possibility to obtain a controlled cleaning, minimizing the use of organic solvents for the removal of hydrophobic coherent layers onto a surface. The use of emulsions combines the detergency and surface active properties of the surfactant with the synergistic solving action of the organic solvent. Typically, microemulsions are engineered and preferred to emulsion due to their thermodynamic stability. The first successful use of microemulsion to art conservation is reported for the frescoes by Masaccio and Masolino (Brancacci Chapel in Florence, Italy).[1] In the recent years, several formulations were proposed, with the aim of solving specific cleaning issues, the main of which are selective and controlled removal of undesired materials, sustainable products as well as reducing the risk of surfactant/cleaning agents residuals on the artwork surface.[2–5] Particular attention is devoted to the uncontrolled spreading and penetration of the formulations that can lead to unpredictable damage effects. To overcome these issues, alternatives for emulsion stabilizers and gel forming strategies should be considered. In this regards, Pickering emulsion could represent a perspective approach.

Pickering emulsions are stabilized with solid particles instead of surfactants and they exhibit high stability due to their opposition to Oswald ripening and coalescence phenomena.[6] Among solid inexpensive and sustainable stabilizers, clay minerals with variable hollow tubular morphology are very promising. Halloysite nanotubes (HNTs) were very efficient in oil-in-water emulsion stabilization so that it was proposed for oil remediation technology.[7,8] In this respect, HNTs represent the great advantage to be easily dispersed in water media without time-consuming exfoliation procedures needed for other platy clays. Halloysite nanotubes can be used in water purification,[9,10,11] catalysis, drug delivery,[12,13,14,15,16] packaging[17,18,19,20] and in conservation of cultural heritage as consolidant agents[21,22] due to their versatile surface chemistry and interesting colloidal properties.[23,24,25] Very recently, the combination of HNTs with anionic surfactants generated inorganic micelles with solubilization ability toward hydrophobic payloads.[10,26,27] Additionally, HNTs are no toxic for cells, yeast and multicellular organisms.[13,28–32] HNTs are quite polydisperse in size with characteristic sizes largely dependent on the deposit. Their typical length is of ca. 1 μm while the external diameter and the lumen range between 50-80 nm and 10-15 nm, respectively.[33–36]

As concerns the thickener additives to increase the viscosity of the emulsion, different biopolymers are commonly used in conservation such as cellulose ethers and other polysaccharides (agar, xanthan gum). These rigid gels allow minimizing the amount of residues left after the application.[37]

Here, we propose a new strategy for designing Pickering emulsion based on Halloysite nanotubes and exploring chitosan and pectin as thickener additives. These two biopolymers represent very abundant and low cost materials and their use is in agreement with the idea of circular economy being waste of food industry. Nanocomposite films of halloysite nanotubes in combination with pectin and chitosan have been considered promising for sustainable packaging applications, and tissue engineering.[15,38–41] Their use as thickeners can have an influence in the stabilization/destabilization and detergency ability of the Pickering emulsion.

Experimental

Materials

Citrus Pectin (degree of methyl esterification 24%, Mw = 30-100 Kg mol^{-1}), n-decane, Ba(OH)$_2$, NaOH, Chitosan (75-85% deacetylated, Mw = 50-190 Kg mol^{-1}), glacial acetic acid and halloysite (HNT) are from Sigma. All the products were used without further purification. Water from reverse osmosis with a specific resistivity greater than 1 MΩ cm was used was used.

Pickering emulsion preparation

HNTs were dispersed in water at 1.0%, after ultrasonication (10 min), the dispersion was kept under stirring overnight. n-Decane was added to the dispersion at a oil:water ratio of 1:3. Emulsion was obtained by vortex mixing for 2 min. The obtained emulsion was creamy-white and stable for more than a month at room temperature.

Pectin and Chitosan gel preparation

Pectin was dissolved in water (5 wt %) under magnetic stirring at 70 °C. The solution was left to equilibrate under magnetic stirring overnight at room temperature. Then, an appropriate amount of HNTs and n-Decane were added to the pectin solution following the protocol described for the Pickering emulsion preparation. The gel phase was obtained by adding Ba(OH)$_2$ saturated solution (ca. 47 g dm^{-3}) under magnetic stirring. The final barium hydroxide concentration in the gel was 0.4 wt% and the gel pH was 8.2.

Chitosan was dissolved at 2 wt% in acetic acid (1 wt%) aqueous solution under magnetic stirring at room temperature. The solution was kept under magnetic stirring overnight at room temperature. Pickering emulsion was prepared based on the previously described protocol by adding appropriate amounts of HNTs and n-Decane to the chitosan solution. The gel phase was obtained by adding dropwise Na(OH) solution (1.5 M) under magnetic stirring. The final sodium hydroxide concentration in the gel was ca. 0.3 M and the gel pH was 12.1.

Methods

The surface morphology of the halloysite nanotubes was studied by using a microscope ESEM FEI QUANTA 200F. Before each SEM experiment, the surface of the sample was coated with gold in argon by means of an Edwards Sputter Coater S150A to avoid charging under electron beam. The measurements were carried out in high vacuum mode (<6×10^{-4} Pa) for simultaneous secondary electron, the energy of the beam was 20 kV and the working distance was 10 mm. Minimal electron dose condition was set to avoid damage of the sample. Fluorescence spectra of pectin based gel and

marble surface were recorded using Fluoromax 4 (Jobin-Yvon) spectrofluorometer (30° angle geometry). Excitation wavelength was fixed at 313 nm, while the emission spectra were registered from 330 to 600 nm. Water contact angle measurements were performed with an apparatus equipped with a CCD camera with high-resolution (OCA 20, Data Physics Instruments). SCA 20 software (Data Physics Instruments) was used for data analysis. The water contact angle just after the deposition (θ_i) was measured by placing a droplet of 10.0 ± 0.5 µL onto the solid surface. Each measurement was repeated three times at least, and the average values are reported. The color parameter changes of the marble surface upon cleaning was followed by the image analysis according to literature,[42] acquiring by a flatbed digital scanner images as RGB files at a spatial resolution of 1200 dpi and converting the image to Lab coordinates by means of ImageJ software. The color change expressed as ΔE parameter was calculated as average value in an area of ca. 1cm × 1cm. The "cleaned" marble surface was defined for water contact angle and color change experiments by considering the surface after polishing with sandpaper. The surface tension experiments were carried out by using a programmable tensiometer (KSV Sigma 70) equipped with a Wilhemy plate at 25.0 ± 0.1 °C. The platinum plate was lowered to the surface of the solution, and the downward force to the plate was measured. Surface tension was obtained as the force divided by the perimeter of the plate. The optical micrographs were taken with an

Optika polarizing microscope at room temperature.

Confocal laser scanning microscopy (CLSM) images were taken using a LSM 780 instrument (Carl Zeiss). The emulsion was first vortexed for 20 s, then a droplet (7µL) of the emulsion was placed onto a glass slide and sandwiched by a glass coverslip. The fluorescence was excited using a 488 nm argon laser, images were processed using ZEN Black software. Dark-field and corresponding fluorescence microscopy images were captured using an Olympus BX51 upright microscope equipped with 100x fluorite objective, a Cytoviva® high annular aperture dark-field condenser and DAGE CCD camera. Fluorescence in sample was excited using an X-cite 120Q wide-field fluorescence excitation light source (Excelitas Technologies) a Cytoviva® Dual Mode Fluorescence system, exposure time was 300 µs. Images were captured using Exponent 7 software (Dage-MTI). Reflected light spectra were recorded in 400-1000 nm with a 2.0 nm spectral resolution using a Specim spectrometer and Pixelfly USB (PCO) CCD camera. ENVI 4.8 software was used to process the spectra obtained. Atomic force microscopy (AFM) images were obtained using a Dimension Icon instrument (Bruker) equipped with ScanAsyst-Air (Bruker) probes (nominal length 115 µm, tip radius 2 nm, spring constant $0.4 \, \text{n} \, \text{m}^{-1}$) (Bruker) were used throughout. AFM raw data obtained were processed using Nanoscope Analysis software v 1.7 (Bruker).

Results and Discussion

Characterization of Pickering emulsion

The Pickering emulsions in gel were imaged by an optical microscope. The Oil/HNTs/water Pickering emulsion clearly showed the presence of oil droplets having a radius ranging between 20 to 40 μm (Figure 1). This value is in agreement with that reported for similar system in the literature.[7] Interestingly, the presence of biopolymer (both chitosan and pectin) and the formation of gel phase affected both the stability and the distribution of the oil droplets in the Pickering emulsions. As shown in Figure 1, Pickering emulsion in chitosan gel possesses a clear phase separation although the oil droplet are still present. In contrast, oil droplets are homogenesly dispersed in pectin gel phase. Compared to oil/HNTs/water Pickering emulsions, the droplet size distribution is shifted towards smaller value in the presence of pectin gel. Therefore, pectin simultaneously acts as gelling agent and emulsion stabilizer. The confocal imaging confirms the optical observations. It should be noted that the detected fluorescence signal is due to pectin auto fluorescence and it shows an accumulation of the biopolymer close to the droplet (Figure 2). Based on the collected images, one cannot exclude that pectin is also penetrating the droplets. Dark-field images and hyperspectral data analysis provided a deeper understanding on the halloysite nanotubes location within the emulsion system. Comparing correlative dark-field and fluorescence microscopy images of the emulsion droplets in water one can see the intensive light scattering originating from halloysite covering the chitosan gels (Figure 2 a,b) . The reflected light spectra obtained from the droplets is reminiscent of those for pure HNTs and the hyperspectral images indicate the nanotubes interfacial accumulation. In addition, CLSM images were also taken to confirm the morphology and size distribution of the emulsion droplets (Figure 2 d). Atomic force microscopy in nanomechanical PeakForce Tapping mode was applied to investigate the distribution of halloysite nanotubes within the pectin gels (Figure 3). As one can see, the individual nanotubes are distributed diffusely, some being embedded into the pectin matrix, while the others reside on the top of the pectin layer, as confirmed by non-specific adhesion measurement. Interestingly, pectin areas exhibited a much higher (ca. 25-27 nN) non-specific adhesion towards the AFM probe tip that surface-exposed HNTs (5-12 nN).
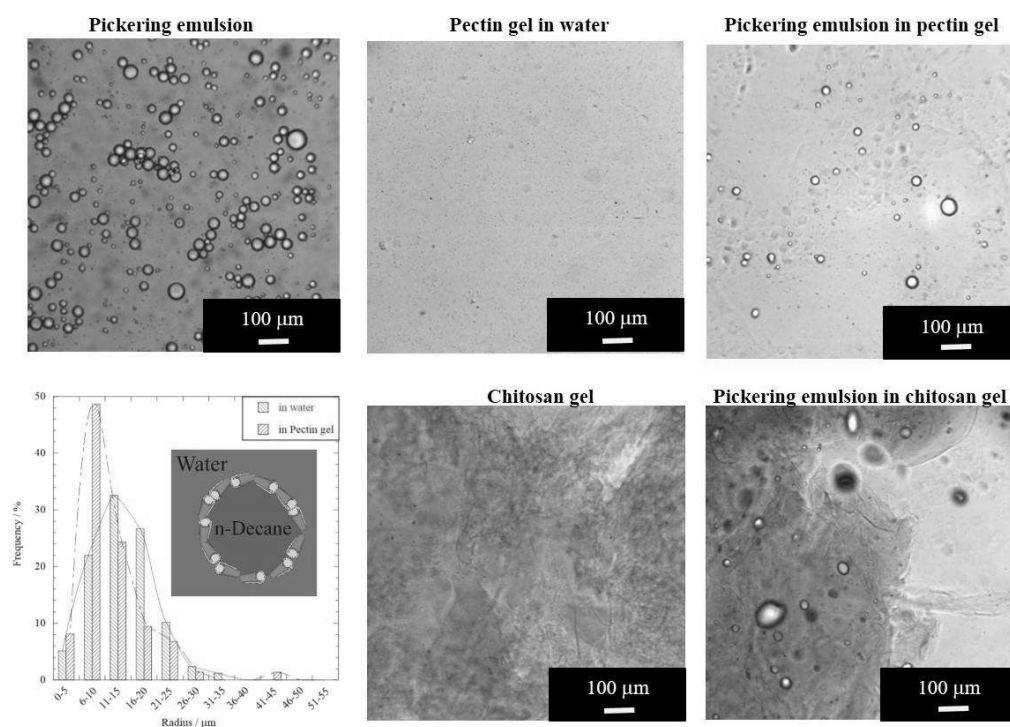
Figure 1. Optical images of Pickering emulsions and size distribution for oil droplets.
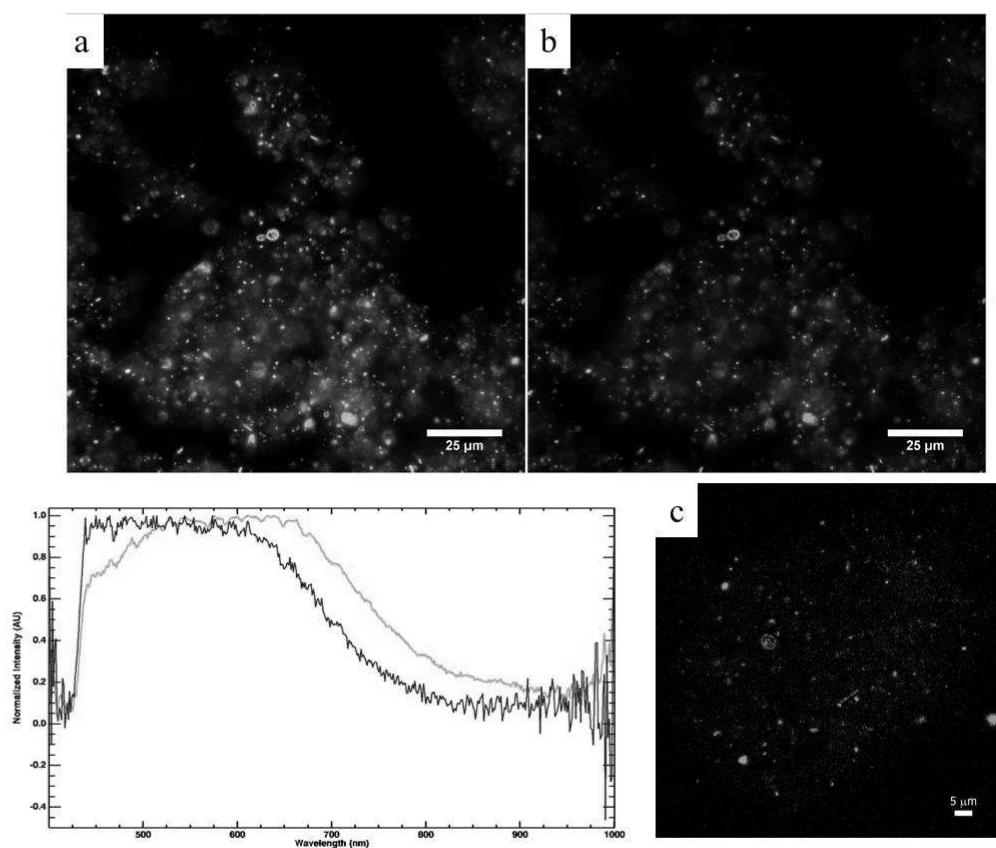

Figure 2. Dark-field (a) and corresponding transmitted light fluorescence (b) images of Pickering emulsions, reflected light spectra (green curve - pectin; blue curve - halloysite) and confocal imaging (c) of Pickering emulsion in pectin gel.
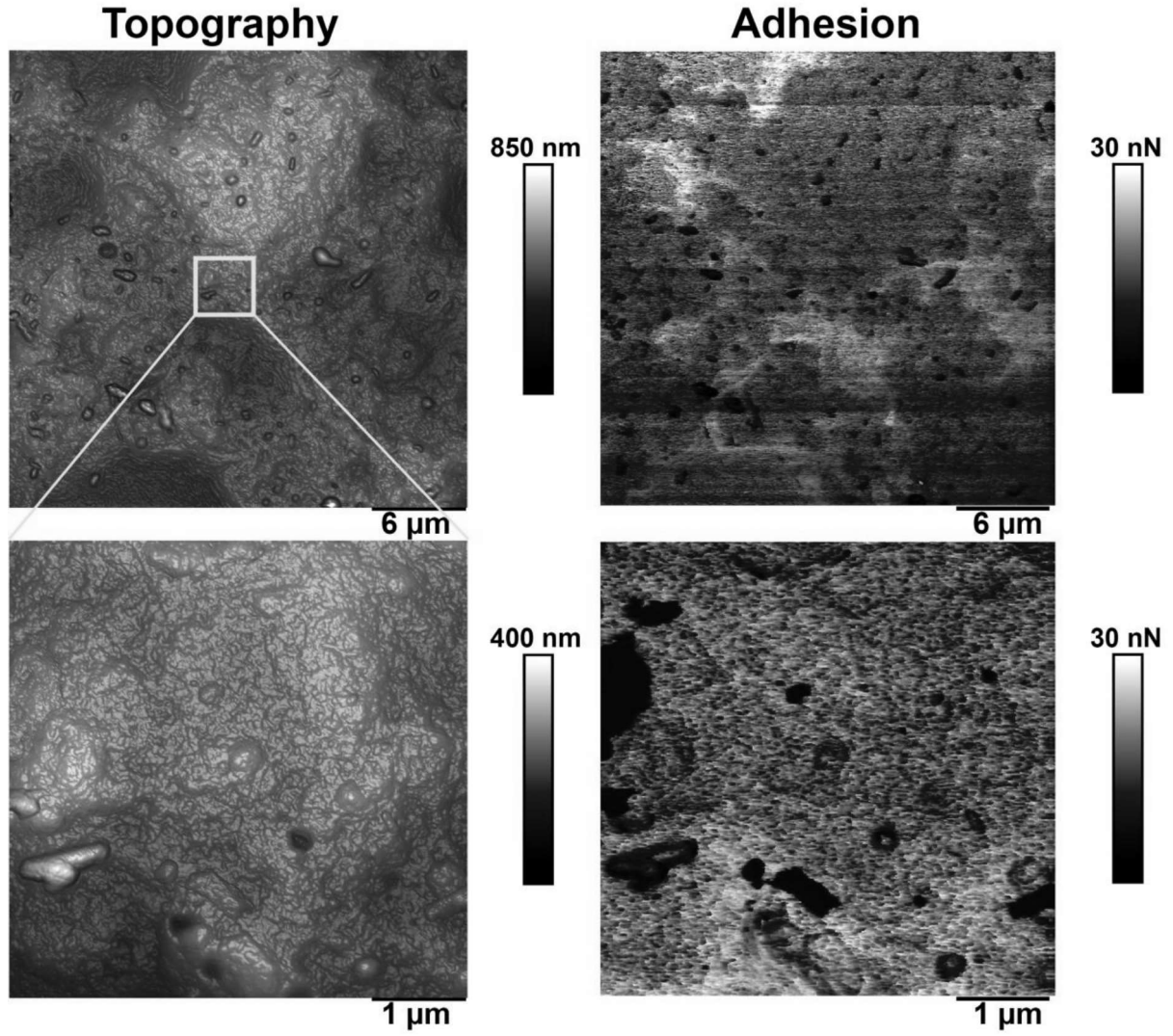
Figure 3. Atomic force microscopy images of dried Pickering emulsion in pectin gel taken in PeakForce Tapping nanomechanical mode.

A deeper investigation on the stability of the Pickering emulsion can be achieved by studying the interfacial activity of clay nanotubes in aqueous media. The free energy change (ΔGd) when the nanotube is detached from oil/water interface and submerged into the aqueous phase is given by[7]

$$\Delta Gd = 2rL\gamma_{ow} (\sin\theta-\theta\cos\theta-rL^{-1}\theta\cos\theta+rL^{-1}\cos^2\theta\sin\theta) \tag{1}$$

where r and L are radius and length of the nanotubes, γ_{ow} is the tension of oil-water interface and θ the three-phase contact angle measured with the tablet method (Figure 4).[43] Calculation was

performed by using the r and L values from literature.[35] The measured γ_{ow} and θ values are collected with the calculated ΔGd in Table 1. In all cases, HNTs are strongly bond at the interface being that the detaching energy is much larger than the thermal energy. For n-dodecane/HNTs/water Pickering emulsion, Owosen et al[7] reported a detaching energy value equals to $(3.45\times10^4)KT$, which is consistent with our result (Table 1). It is clearly detected that both biopolymers enhance the HNTs affinity towards the oil/water interface as evidenced by the ΔGd results. This effect is stronger for pectin addition, which induced a ΔGd increase larger than one order of magnitude with respect to that of n-decane/HNTs/water system.The stabilizing effect of pectin is consistent with its accumulation at the oil/water interface evidenced by confocal imaging. Based on the thermodynamic and morphological results, we can conclude that pectin is the better biopolymer to prepare stable emulsion. Interestingly, the addition of dications can allow to increase the viscosity of the Pickering emulsion formed in pectin gel.
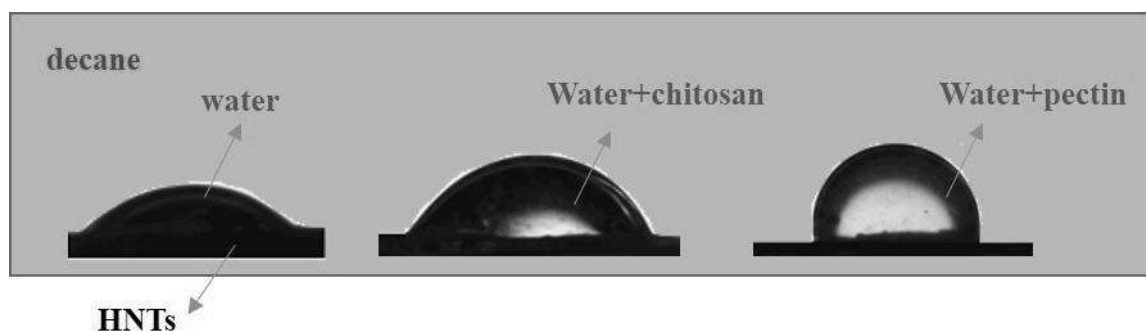

Figure 4. Contact angle experiment for water droplet in decane media onto HNTs tablet surface.

Table 1. Interfacial properties for n-decane/HNTs/aqueous phase systems.

Aqueous phase	γ_{ow} / mN m^{-1}	θ / °	$\Delta Gd/KT$
water	35.6±0.6	37±1.2	7.0×10^4
Water+chitosan 2wt%	35.0±1.0	59.7±1.5	27×10^4
Water+pectin 5 wt%	27.5±0.9	117.1±0.8	125×10^4

Cleaning of marble surface

We carried out a test on the ability of Pickering emulsion in pectin gel for the removal of wax from a marble surface. A thin layer of ca. 100 μm of beeswax was deposited on marble samples. After

this treatment the surface color appeared altered and it turned from white to brownish. The choice of wax has a double purpose: i) it can be considered as a model system for an hydrophobic layer, ii) it was used as protective layer for marble artifacts in the past and nowadays its removal is a first step for a cleaning protocol in Conservation of Cultural Heritage. The efficacy of the wax removal from a marble surface was estimated by monitoring both the water contact angle and the colorimeter parameters of the surface as a function of gel application time. Figure 5 shows the macroscopic cleaning action of the gel application on the marble surface. As concerns the colorimeter parameters, it is typically accepted that $\Delta E < 2.3$ indicates undistinguished colors for human eyes. As reported in Figure 6, the pectin based gel is more efficient than chitosan in wax removal. This result is likely related to the structural characteristics of the Pickering emulsions, which presents phase separation and a uniformity in chitosan and pectin gels, respectively. Water contact angle data are sensitive to the cleaning process and they show that the marble surface is free of hydrophobic substances after ca. 50 min of gel application time (Figure 7). Going further, we decided to monitor the presence of pectin residuals onto the marble surface after the cleaning procedure. To this aim fluorescence spectra were collected before and after surface rinsing with water and a cotton swabs. Results indicated that pectin residuals are below detection limit if a proper water rinsing is performed after gel application (Figure 8).

Finally, the Pickering emulsion in pectin gel was tested in a real artwork. The cherubs of the funeral monument of Placido Caruso from St. Joseph's Chapel in Polizzi Generosa (Italy) was selected, although a very little information about the nature of the coating was available, the surface appeared far from the typical white of marble likely due to coherent layer of dust. Moreover, the hydrophobic nature of the deposit is proved by the low and inefficient cleaning action of water applied with a cotton swab. Thus, cleaning was carried out by means of the Pickering emulsion in pectin gel phase. The optical photos before and after the treatment (Figure 9) show the promising results in terms of whitening and controlled cleaning of the surface after 10 min contact time.
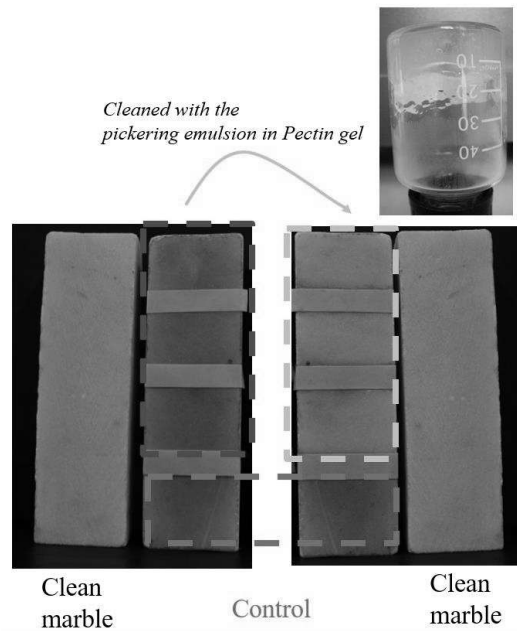
Figure 5. Optical photo of marble sample before and after Pickering emulsion in pectin gel application.
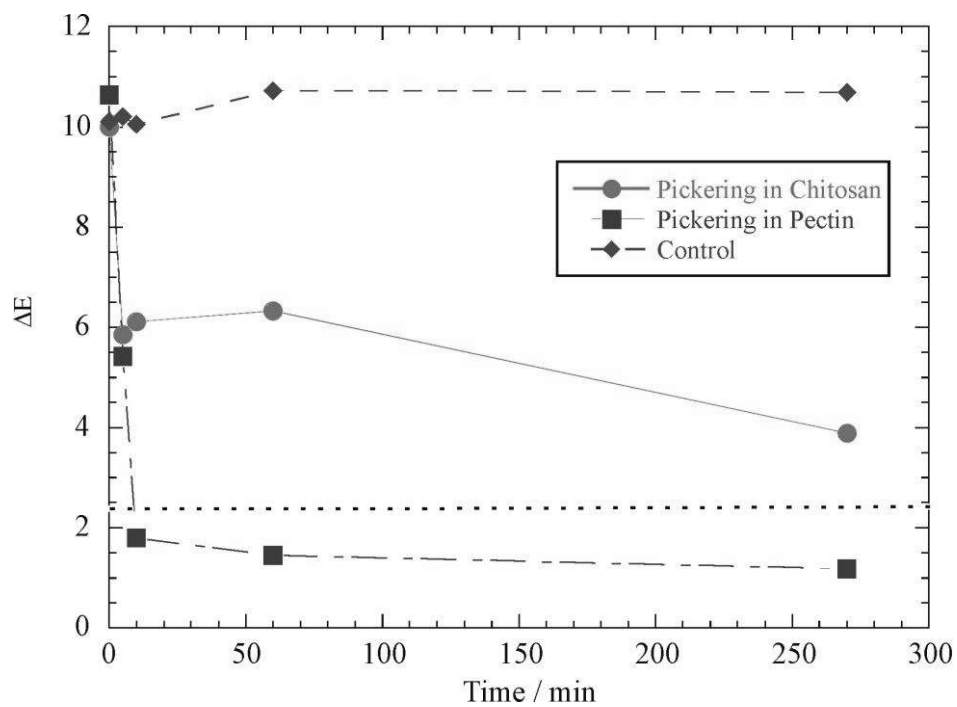

Figure 6. Color difference parameter for marble surface during cleaning with Pickering in Pectin and Chitosan gels as a function of the gel application time. Control refers to untreated region. Dashed line is the contact angle on polished marble surface.
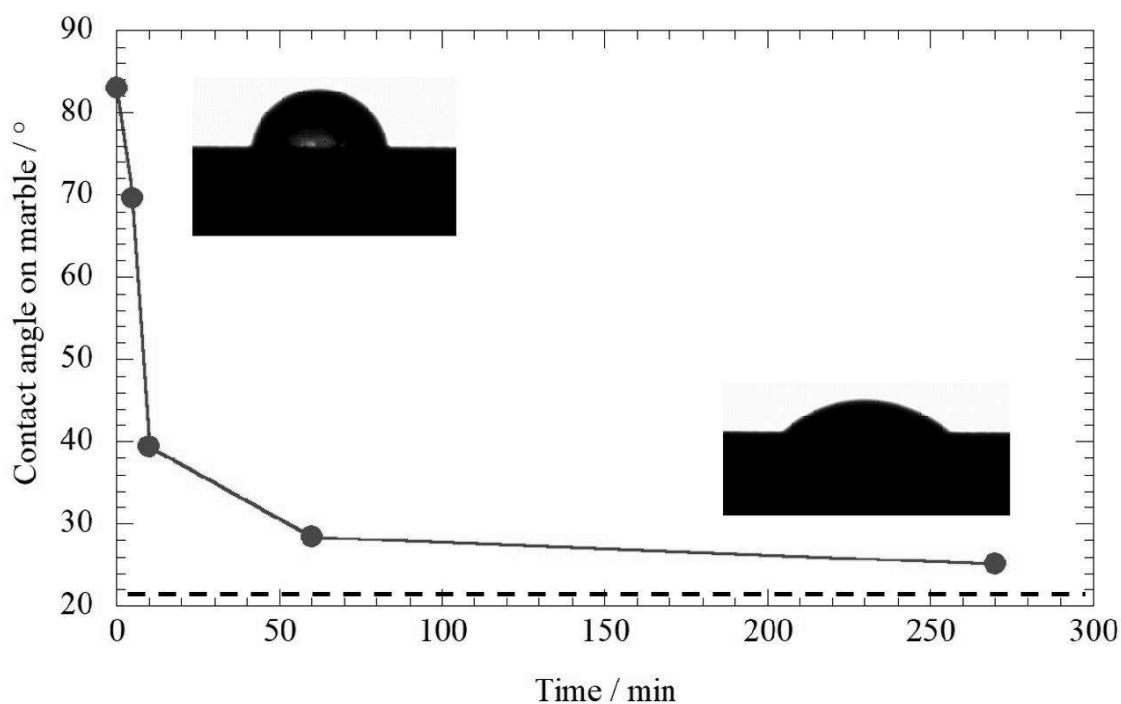
Figure 7. Water contact angle onto marble surface during cleaning with Pickering in Pectin gel as a function of the gel application time. Dashed line is the contact angle on polished marble surface.
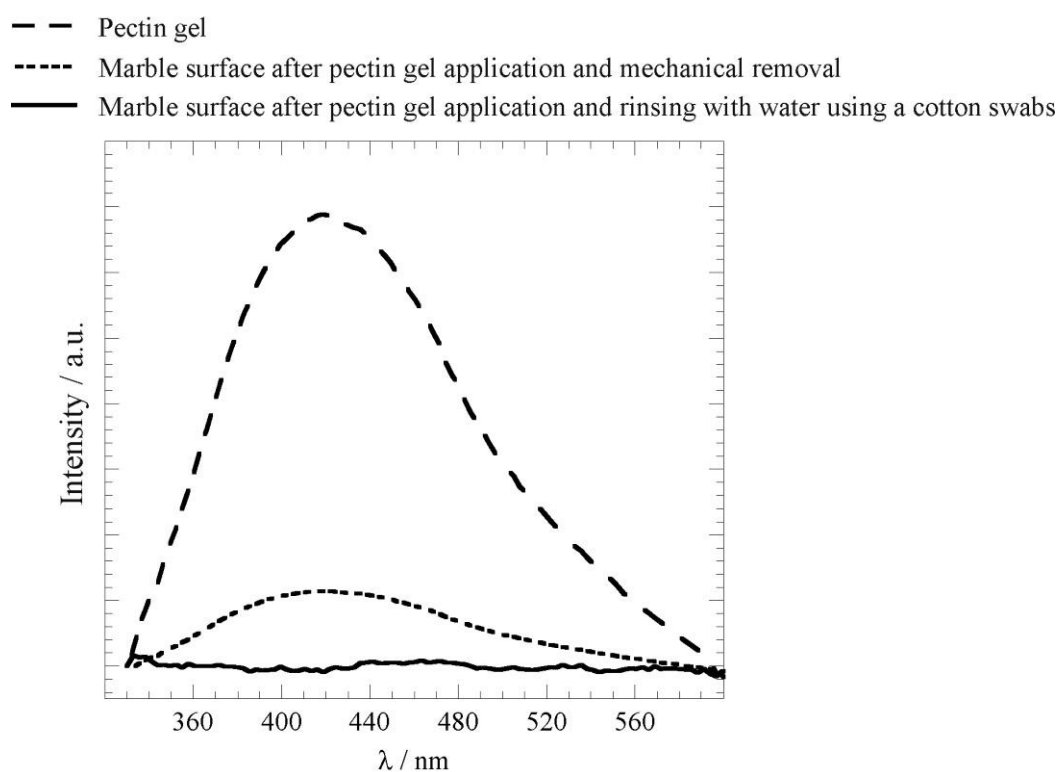

Figure 7. Fluorescence spectra from pectin gel, marble surface after cleaning with Pickering in Pectin gel and mechanical or water rinsing for gel removal.
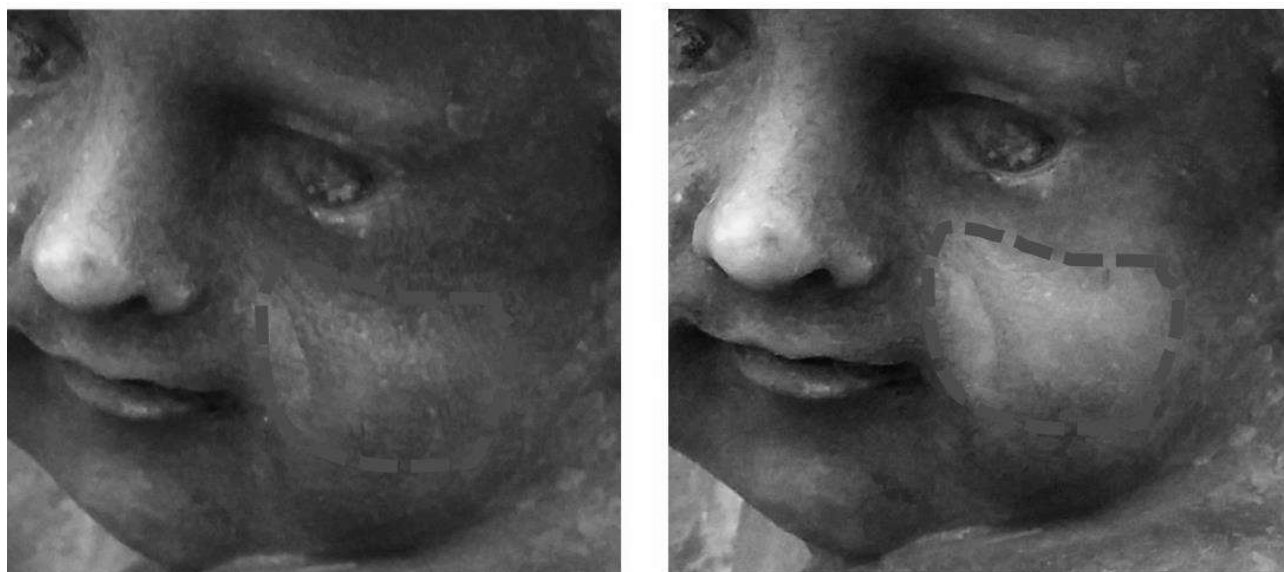
Figure 9. Application of the Pickering in Pectin gel system on cherubs of the funeral monument of Placido Caruso (Polizzi Generosa, Italy). Left hand side: Before cleaning. Right hand side: After cleaning. In the dashed box, the cleaning region.

Conclusions

Pickering emulsions gels were successfully fabricated by the combination of halloysite nanotubes and biopolyelectrolites (pectin and chitosan). We observed that the adsorption of the nanotubes at the water/oil interface is strongly favored from the thermodynamic point of view and it provides a steric barrier against drop coalescence. The synergistic stabilization of emulsions was evidenced by halloysite and biopolymers (chitosan or pectin). Pectin allowed us to obtain a stable and uniform gel from the Pickering emulsion and the polymer/nanotubes accumulation at the oil droplet surface was imaged. Therefore, a oil pool dispersed in micro-ranged droplets separated from the continuous water phase by the nanotubes/pectin layer is obtained. The system is very promising in practical applications related to controlled cleaning of stone based artifacts. In particular the dispersion of oil into small droplets will ensure a non-aggressive and safe cleaning agent while the gel nature provides a well defined area of application. In addition to the encouraging cleaning performance, the prepared formulations follows a sustainable receipt being all components, with the exception of the oil phase, from natural sources. The large amount availability at low cost of halloysite nanotubes and pectin additionally renders conversion to large scale applications feasible. Finally, the main contribution that this work offers in the field of nanomaterials for the cleaning of artworks is the introduction of the Pickering emulsion in gel phase by using biocompatible ingredients.

References

(1)   Borgioli, L.; Caminati, G.; Gabrielli, G.; Ferroni, E. Removal of Hydrophobic Impurities from Pictorial Surfaces by Means of Heterogeneous Systems. *Sci Technol Cult Herit* **1995**, *4* (2), 67–74.

(2)   Casoli, A.; Di Diego, Z.; Isca, C. Cleaning Painted Surfaces: Evaluation of Leaching Phenomenon Induced by Solvents Applied for the Removal of Gel Residues. *Environ. Sci. Pollut. Res.* **2014**, *21* (23), 13252–13263. https://doi.org/10.1007/s11356-014-2658-5.

(3)   Baglioni, M.; Montis, C.; Brandi, F.; Guaragnone, T.; Meazzini, I.; Baglioni, P.; Berti, D. Dewetting Acrylic Polymer Films with Water/Propylene Carbonate/Surfactant Mixtures – Implications for Cultural Heritage Conservation. *Phys. Chem. Chem. Phys.* **2017**, *19* (35), 23723–23732. https://doi.org/10.1039/C7CP02608K.

(4)   Baglioni, M.; Jàidar Benavides, Y.; Berti, D.; Giorgi, R.; Keiderling, U.; Baglioni, P. An Amine-Oxide Surfactant-Based Microemulsion for the Cleaning of Works of Art. *J. Colloid Interface Sci.* **2015**, *440*, 204–210. https://doi.org/10.1016/j.jcis.2014.10.003.

(5)   Baglioni, P.; Berti, D.; Bonini, M.; Carretti, E.; Dei, L.; Fratini, E.; Giorgi, R. Micelle, Microemulsions, and Gels for the Conservation of Cultural Heritage. *Adv. Colloid Interface Sci.* **2014**, *205*, 361–371. https://doi.org/10.1016/j.cis.2013.09.008.

(6)   Cunningham, V. J.; Giakoumatos, E. C.; Ireland, P. M.; Mable, C. J.; Armes, S. P.; Wanless, E. J. Giant Pickering Droplets: Effect of Nanoparticle Size and Morphology on Stability. *Langmuir* **2017**, *33* (31), 7669–7679. https://doi.org/10.1021/acs.langmuir.7b01383.

(7)   Owoseni, O.; Nyankson, E.; Zhang, Y.; Adams, S. J.; He, J.; McPherson, G. L.; Bose, A.; Gupta, R. B.; John, V. T. Release of Surfactant Cargo from Interfacially-Active Halloysite Clay Nanotubes for Oil Spill Remediation. *Langmuir* **2014**, *30* (45), 13533–13541. https://doi.org/10.1021/la503687b.

(8)   von Klitzing, R.; Stehl, D.; Pogrzeba, T.; Schomäcker, R.; Minullina, R.; Panchal, A.; Konnova, S.; Fakhrullin, R.; Koetz, J.; Möhwald, H.; et al. Halloysites Stabilized Emulsions for Hydroformylation of Long Chain Olefins. *Adv. Mater. Interfaces* **2016**, 1600435-n/a. https://doi.org/10.1002/admi.201600435.

(9)   Zhao, Y.; Abdullayev, E.; Vasiliev, A.; Lvov, Y. Halloysite Nanotubule Clay for Efficient Water Purification. *J. Colloid Interface Sci.* **2013**, *406* (0), 121–129. https://doi.org/10.1016/j.jcis.2013.05.072.

(10)   Cavallaro, G.; Lazzara, G.; Milioto, S.; Parisi, F.; Sanzillo, V. Modified Halloysite Nanotubes: Nanoarchitectures for Enhancing the Capture of Oils from Vapor and Liquid Phases. *ACS Appl. Mater. Interfaces* **2014**, *6* (1), 606–612. https://doi.org/10.1021/am404693r.

(11)   Luo, P.; Zhang, J.; Zhang, B.; Wang, J.; Zhao, Y.; Liu, J. Preparation and Characterization of Silane Coupling Agent Modified Halloysite for Cr(VI) Removal. *Ind Eng Chem Res* **2011**, *50* (17), 10246–10252. https://doi.org/10.1021/ie200951n.

(12)   Vergaro, V.; Lvov, Y. M.; Leporatti, S. Halloysite Clay Nanotubes for Resveratrol Delivery to Cancer Cells. *Macromol. Biosci.* **2012**, *12* (9), 1265–1271. https://doi.org/10.1002/mabi.201200121.

(13)   Vergaro, V.; Abdullayev, E.; Lvov, Y. M.; Zeitoun, A.; Cingolani, R.; Rinaldi, R.; Leporatti, S. Cytocompatibility and Uptake of Halloysite Clay Nanotubes. *Biomacromolecules* **2010**, *11* (3), 820–826. https://doi.org/10.1021/bm9014446.

(14)   Massaro, M.; Riela, S.; Lo Meo, P.; Noto, R.; Cavallaro, G.; Milioto, S.; Lazzara, G. Functionalized Halloysite Multivalent Glycocluster as a New Drug Delivery System. *J. Mater. Chem. B* **2014**, *2* (44), 7732–7738. https://doi.org/10.1039/C4TB01272K.

(15)   Liu, M.; Wu, C.; Jiao, Y.; Xiong, S.; Zhou, C. Chitosan-Halloysite Nanotubes Nanocomposite Scaffolds for Tissue Engineering. *J. Mater. Chem. B* **2013**, *1* (15), 2078–2089. https://doi.org/10.1039/C3TB20084A.

(16) Lee, Y.; Jung, G.-E.; Cho, S. J.; Geckeler, K. E.; Fuchs, H. Cellular Interactions of Doxorubicin-Loaded DNA-Modified Halloysite Nanotubes. *Nanoscale* **2013**, *5*, 8577–8585. https://doi.org/10.1039/C3NR02665E.

(17) Cavallaro, G.; Donato, D. I.; Lazzara, G.; Milioto, S. Films of Halloysite Nanotubes Sandwiched between Two Layers of Biopolymer: From the Morphology to the Dielectric, Thermal, Transparency, and Wettability Properties. *J Phys Chem C* **2011**, *115* (42), 20491–20498. https://doi.org/10.1021/jp207261r.

(18) Gorrasi, G.; Pantani, R.; Murariu, M.; Dubois, P. PLA/Halloysite Nanocomposite Films: Water Vapor Barrier Properties and Specific Key Characteristics. *Macromol. Mater. Eng.* **2014**, *299* (1), 104–115. https://doi.org/10.1002/mame.201200424.

(19) De Silva, R. T.; Pasbakhsh, P.; Goh, K. L.; Chai, S.-P.; Ismail, H. Physico-Chemical Characterisation of Chitosan/Halloysite Composite Membranes. *Polym. Test.* **2013**, *32* (2), 265–271. https://doi.org/10.1016/j.polymertesting.2012.11.006.

(20) He, Y.; Kong, W.; Wang, W.; Liu, T.; Liu, Y.; Gong, Q.; Gao, J. Modified Natural Halloysite/Potato Starch Composite Films. *Carbohydr. Polym.* **2012**, *87* (4), 2706–2711. https://doi.org/10.1016/j.carbpol.2011.11.057.

(21) Cavallaro, G.; Milioto, S.; Parisi, F.; Lazzara, G. Halloysite Nanotubes Loaded with Calcium Hydroxide: Alkaline Fillers for the Deacidification of Waterlogged Archeological Woods. *ACS Appl. Mater. Interfaces* **2018**, *10* (32), 27355–27364. https://doi.org/10.1021/acsami.8b09416.

(22) Cavallaro, G.; Lazzara, G.; Milioto, S.; Parisi, F.; Ruisi, F. Nanocomposites Based on Esterified Colophony and Halloysite Clay Nanotubes as Consolidants for Waterlogged Archaeological Woods. *Cellulose* **2017**, *24* (8), 3367–3376. https://doi.org/10.1007/s10570-017-1369-8.

(23) Lvov, Y.; Abdullayev, E. Functional Polymer–Clay Nanotube Composites with Sustained Release of Chemical Agents. *Prog Polym Sci* **2013**, *38* (10–11), 1690–1719. https://doi.org/10.1016/j.progpolymsci.2013.05.009.

(24) Luo, Z.; Song, H.; Feng, X.; Run, M.; Cui, H.; Wu, L.; Gao, J.; Wang, Z. Liquid Crystalline Phase Behavior and Sol–Gel Transition in Aqueous Halloysite Nanotube Dispersions. *Langmuir* **2013**, *29* (40), 12358–12366. https://doi.org/10.1021/la402836d.

(25) Lazzara, G.; Cavallaro, G.; Panchal, A.; Fakhrullin, R.; Stavitskaya, A.; Vinokurov, V.; Lvov, Y. An Assembly of Organic-Inorganic Composites Using Halloysite Clay Nanotubes. *Curr. Opin. Colloid Interface Sci.* **2018**, *35*, 42–50. https://doi.org/10.1016/j.cocis.2018.01.002.

(26) Cavallaro, G.; Grillo, I.; Gradzielski, M.; Lazzara, G. Structure of Hybrid Materials Based on Halloysite Nanotubes Filled with Anionic Surfactants. *J. Phys. Chem. C* **2016**, *120* (25), 13492–13502. https://doi.org/10.1021/acs.jpcc.6b01282.

(27) Cavallaro, G.; Lazzara, G.; Milioto, S. Exploiting the Colloidal Stability and Solubilization Ability of Clay Nanotubes/Ionic Surfactant Hybrid Nanomaterials. *J. Phys. Chem. C* **2012**, *116* (41), 21932–21938. https://doi.org/10.1021/jp307961q.

(28) Fakhrullina, G. I.; Akhatova, F. S.; Lvov, Y. M.; Fakhrullin, R. F. Toxicity of Halloysite Clay Nanotubes in Vivo: A Caenorhabditis Elegans Study. *Environ. Sci. Nano* **2015**, *2* (1), 54–59. https://doi.org/10.1039/C4EN00135D.

(29) Kryuchkova, M.; Danilushkina, A.; Lvov, Y.; Fakhrullin, R. Evaluation of Toxicity of Nanoclays and Graphene Oxide in Vivo: A Paramecium Caudatum Study. *Environ. Sci. Nano* **2016**, *3* (2), 442–452. https://doi.org/10.1039/C5EN00201J.

(30) Shutava, T. G.; Fakhrullin, R. F.; Lvov, Y. M. Spherical and Tubule Nanocarriers for Sustained Drug Release. *Curr Opin Pharmacol* **2014**, *18* (0), 141–148. https://doi.org/10.1016/j.coph.2014.10.001.

(31)   Bellani, L.; Giorgetti, L.; Riela, S.; Lazzara, G.; Scialabba, A.; Massaro, M. Ecotoxicity of Halloysite Nanotube–Supported Palladium Nanoparticles in Raphanus Sativus L. *Environ. Toxicol. Chem.* **2016**, *35* (10), 2503–2510. https://doi.org/10.1002/etc.3412.

(32)   Wang, X.; Gong, J.; Rong, R.; Gui, Z.; Hu, T.; Xu, X. Halloysite Nanotubes-Induced Al Accumulation and Fibrotic Response in Lung of Mice after 30-Day Repeated Oral Administration. *J. Agric. Food Chem.* **2018**, *66* (11), 2925–2933. https://doi.org/10.1021/acs.jafc.7b04615.

(33)   Lvov, Y. M.; Shchukin, D. G.; Mohwald, H.; Price, R. R. Halloysite Clay Nanotubes for Controlled Release of Protective Agents. *ACS Nano* **2008**, *2* (5), 814–820. https://doi.org/doi: 10.1021/nn800259q.

(34)   Pasbakhsh, P.; Churchman, G. J.; Keeling, J. L. Characterisation of Properties of Various Halloysites Relevant to Their Use as Nanotubes and Microfibre Fillers. *Appl. Clay Sci.* **2013**, *74*, 47–57. https://doi.org/10.1016/j.clay.2012.06.014.

(35)   Cavallaro, G.; Chiappisi, L.; Pasbakhsh, P.; Gradzielski, M.; Lazzara, G. A Structural Comparison of Halloysite Nanotubes of Different Origin by Small-Angle Neutron Scattering (SANS) and Electric Birefringence. *Appl. Clay Sci.* **2018**, *160*, 71–80. https://doi.org/10.1016/j.clay.2017.12.044.

(36)   Joussein, E.; Petit, S.; Churchman, G. J.; Theng, B.; Righi, D.; Delvaux, B. Halloysite Clay Minerals — a Review. *Clay Miner.* **2005**, *40* (4), 383–426.

(37)   Mazzuca, C.; Micheli, L.; Cervelli, E.; Basoli, F.; Cencetti, C.; Coviello, T.; Iannuccelli, S.; Sotgiu, S.; Palleschi, A. Cleaning of Paper Artworks: Development of an Efficient Gel-Based Material Able to Remove Starch Paste. *ACS Appl. Mater. Interfaces* **2014**, *6* (19), 16519–16528. https://doi.org/10.1021/am504295n.

(38)   Gorrasi, G. Dispersion of Halloysite Loaded with Natural Antimicrobials into Pectins: Characterization and Controlled Release Analysis. *Carbohydr. Polym.* **2015**, *127*, 47–53. https://doi.org/10.1016/j.carbpol.2015.03.050.

(39)   Gorrasi, G.; Bugatti, V.; Vittoria, V. Pectins Filled with LDH-Antimicrobial Molecules: Preparation, Characterization and Physical Properties. *Carbohydr. Polym.* **2012**, *89* (1), 132–137. https://doi.org/10.1016/j.carbpol.2012.02.061.

(40)   Liu, M.; Zhang, Y.; Wu, C.; Xiong, S.; Zhou, C. Chitosan/Halloysite Nanotubes Bionanocomposites: Structure, Mechanical Properties and Biocompatibility. *Int. J. Biol. Macromol.* **2012**, *51* (4), 566–575. https://doi.org/10.1016/j.ijbiomac.2012.06.022.

(41)   Bertolino, V.; Cavallaro, G.; Lazzara, G.; Milioto, S.; Parisi, F. Halloysite Nanotubes Sandwiched between Chitosan Layers: Novel Bionanocomposites with Multilayer Structures. *New J. Chem.* **2018**, *42* (11), 8384–8390. https://doi.org/10.1039/C8NJ01161C.

(42)   Rizzo, G.; Ercoli, L.; Megna, B. Effectiveness of Preservative Treatments on Coloured Ruditic Building Stones. *Strain* **2009**, *45* (5), 424–432. https://doi.org/10.1111/j.1475-1305.2008.00547.x.

(43)   Abdullayev, E.; Price, R.; Shchukin, D.; Lvov, Y. Halloysite Tubes as Nanocontainers for Anticorrosion Coating with Benzotriazole. *ACS Appl. Mater. Interfaces* **2009**, *1* (7), 1437–1443. https://doi.org/10.1021/am9002028.